

Research Article

Broadband Dielectric Properties of $\text{Fe}_2\text{O}_3\cdot\text{H}_2\text{O}$ Nanorods/Epoxy Resin Composites

Darya Meisak ^{1,2}, Jan Macutkevicius ¹, Dzmitry Bychanok^{2,3}, Algirdas Selskis⁴, Juras Banyys¹ and Polina Kuzhir^{2,3}

¹Physics Faculty, Vilnius University, Vilnius 00122, Lithuania

²Research Institute for Nuclear Problems, Belarusian State University, Minsk 220030, Belarus

³Tomsk State University, Tomsk 634050, Russia

⁴Center for Physical Sciences and Technology, Vilnius 10257, Lithuania

Correspondence should be addressed to Darya Meisak; dariameysak@gmail.com

Received 29 May 2018; Revised 5 October 2018; Accepted 31 October 2018; Published 16 January 2019

Academic Editor: Ovidiu Ersen

Copyright © 2019 Darya Meisak et al. This is an open access article distributed under the Creative Commons Attribution License, which permits unrestricted use, distribution, and reproduction in any medium, provided the original work is properly cited.

A series of polymer composites based on epoxy resin with a 5–40 vol.% concentration of goethite ($\text{Fe}_2\text{O}_3\cdot\text{H}_2\text{O}$) nanorods was produced. The electrical percolation threshold in these composites was determined as 30 vol.% of nanorods. The dielectric properties of the composites both below and above the percolation threshold were studied in a wide temperature (200 K–450 K) and frequency (from Hz to THz) ranges. The dielectric properties of composites below the percolation threshold are mainly determined by the relaxation in a pure polymer matrix. The electrical properties of composites above the percolation threshold are determined by the percolation network, which is formed by the goethite nanorods inside the polymer matrix. Due to the finite conductivity of the epoxy resin, the electrical conductivity at high temperatures occurs in the composites both above and below the percolation threshold.

1. Introduction

Nowadays, there is a great interest in polymer composite materials filled with various nanoparticles, caused by the ability to control their properties at the nanoscale and as a consequence to apply them in different functional devices. Electrically conductive polymer composites based on both organic and inorganic nanofillers attract the attention of scientists because of their potential applications, such as anti-static materials [1] and electromagnetic coatings [2], solar cells and biosensors [3], electromagnetic shielding, and absorption of radiation in different frequency ranges [4].

Due to the low percolation threshold, as well as their unique electrical, thermal, and mechanical properties, various carbon fillers are popular and already studied quite well in recent years [5–8]. However, materials based on metal and metal oxide nanoparticles are also gaining popularity because of their wide range of applications, from catalysis to nanoelectronics [9]. The range of

their potential applications, in particular, iron oxide nanoparticles, expands even more if one considers that in addition to dielectric properties, they can have magnetic and ferromagnetic properties. Then, these particles can also be applied in such areas as magnetic resonance imaging, tissue engineering, and drug delivery and also as hyperthermia agents [10]. Particularly, nanowires, nanorods, and others are interesting composites with high aspect ratio magnetic particles [11, 12]. However, investigations of polymeric composites with goethite ($\text{Fe}_2\text{O}_3\cdot\text{H}_2\text{O}$) nanorods are very rare enough [13]. Moreover, the investigations of goethite and siloxane composites show the relatively small dielectric permittivity value [13]. Therefore, it is important to determine the electrical percolation threshold in composites with goethite nanorods and find the relation between the electrical percolation threshold and composite preparation technology.

The aim of this paper is devoted to the study of the dielectric properties of epoxy resin composites filled with goethite ($\text{Fe}_2\text{O}_3\cdot\text{H}_2\text{O}$) nanorods, which have the big

(about 5) aspect ratio and particular magnetic properties (please see for example [14]).

2. Materials and Methods

Commercial Epikote 828 epoxy resin and a triethylenetetramine hardener (TETA) were used to prepare the composites. The used resin allows the easy dispersion of various additives and shows high mechanical and chemical resistance [1]. The commercially available goethite ($\text{Fe}_2\text{O}_3 \cdot \text{H}_2\text{O}$ alpha, 98%, 50 nm \times 10 nm) nanorod powder was used as a filler [15]. This kind of nanomaterial is widely used in coating, plastic, paint, and pharmaceutical fields. It is a yellow powder with a rod-shaped structure, which is easily dispersed in the polymer matrix and enables the production of composites with high volume concentrations. The surface of $\text{Fe}_2\text{O}_3 \cdot \text{H}_2\text{O}$ nanorod powder was observed by scanning electron microscopy (SEM) using a Helios NanoLab 650 microscope. The SEM image of $\text{Fe}_2\text{O}_3 \cdot \text{H}_2\text{O}$ nanorods is shown in Figure 1. It can be determined that the aspect ratio of nanorods is close to 5.

$\text{Fe}_2\text{O}_3 \cdot \text{H}_2\text{O}$ /epoxy resin composites were produced by the standard procedure for filler dispersion in a polymer matrix, described in detail in [16–18]. Different samples with different concentrations of $\text{Fe}_2\text{O}_3 \cdot \text{H}_2\text{O}$ (namely, 0, 5, 10, 20, 30, and 40 vol.%) were obtained. During the first stage of the procedure, the particles were mechanically crushed and stirred in ethanol during 30 minutes. The particles were, then, dispersed in ethanol with an ultrasonic bath for 1 hour. The resulting dispersion was mixed with the epoxy resin and underwent ultrasonication by probe for 2 hours. Then, ethanol was removed by evaporation and TETA (triethylenetetramine) hardener was added to the resulting mixture (epoxy resin and $\text{Fe}_2\text{O}_3 \cdot \text{H}_2\text{O}$ particles) and mechanically mixed for several minutes. The hardener was added in a ratio of 1 : 10 with respect to the epoxy resin. After that, the mixture was poured into molds, kept for 20 hours at room temperature, and then placed for 2 hours in an oven at a temperature of 100°C for the final polymerization step. The above-presented composite preparation procedure parameters (for example, the stirring time) were experimentally determined as optimal for the best $\text{Fe}_2\text{O}_3 \cdot \text{H}_2\text{O}$ nanorod dispersion in epoxy resin matrix.

The complex dielectric permittivity in the frequency range from 20 Hz to 1 MHz was measured using a LCR meter HP4284A. Each measurement was followed by heating to 450 K and then cooling to 200 K. Dielectric measurements in the frequency range from 1 MHz to 3 GHz were performed using a vector network analyzer Agilent 8714ET. Home-made waveguide spectrometer was used for microwave measurements in the frequency range from 24 to 39 GHz. Thin-rod method was used in the waveguide [19]. A terahertz time-domain spectrometer (Ekspla Ltd.) based on a femtosecond laser was used in the terahertz frequency range from 100 GHz to 3 THz. The spectrometer is based on a femtosecond fiber laser (wavelength 1 μm , pulse duration less than 150 fs) and a GaBiAs photoconductive terahertz emitter and detector [20]. All measurements above 1 MHz were made only at room temperature and only for composites

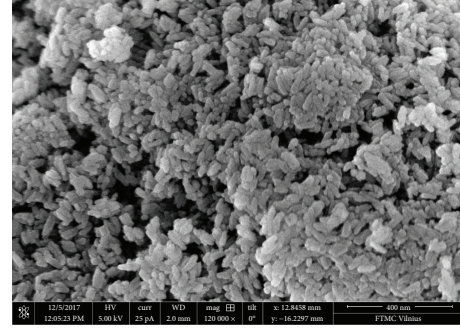


FIGURE 1: Scanning electron microscopy image of $\text{Fe}_2\text{O}_3 \cdot \text{H}_2\text{O}$ nanorods.

above the percolation threshold. Up to 10 samples were tested for each concentration measured under the same heating/cooling conditions, from which the average values were calculated and those in the present paper.

The surface of $\text{Fe}_2\text{O}_3 \cdot \text{H}_2\text{O}$ /epoxy resin composite powder was also observed by scanning electron microscopy (SEM) using Helios NanoLab 650 microscope (see Figure 2). It can be concluded that nanorods are dispersed very well.

3. Results and Discussion

3.1. Electrical Percolation Threshold. The concentration dependence of the complex dielectric permittivity for $\text{Fe}_2\text{O}_3 \cdot \text{H}_2\text{O}$ /epoxy resin composites at room temperature and 129 Hz frequency is shown in Figure 3(a). The addition of nanorods into the polymer matrix leads to an increased dielectric permittivity according to the power law of percolation in the form $\epsilon \propto (p_c - p)^{-t}$, where p is the filler concentration and p_c is the minimum concentration of the filler at which a conducting network inside the composite is generated (percolation threshold) [17, 21]. Approximation of the real part of the dielectric permittivity according to the percolation law is shown in Figure 3(b). This calculation indicates that the electrical percolation for our composite is reached when the filler concentration is 30 vol.%. This is also confirmed by the conductivity plateau in conductivity spectra for composites with 30 vol.% and 40 vol.%, while for lower filler concentrations, this plateau is absent. In order to increase the determination accuracy of p_c , many more samples with different $\text{Fe}_2\text{O}_3 \cdot \text{H}_2\text{O}$ nanorod concentrations close to the critical value are needed. The obtained percolation threshold value is lower than predicted by Monte Carlo calculations in a three dimensional space ~ 31.2 vol.% [22, 23].

3.2. Temperature Dependence of Complex Dielectric Permittivity. The temperature dependence of the complex dielectric permittivity at 129 Hz for all the studied composites is shown in Figure 4. At low temperature composites below the percolation threshold (less than 30 vol.%), it shows a dielectric permittivity close to pure epoxy resin permittivity and it is almost independent of temperature. The imaginary part is quite noisy, because its values are of the same order as the measurement's accuracy at these temperatures.

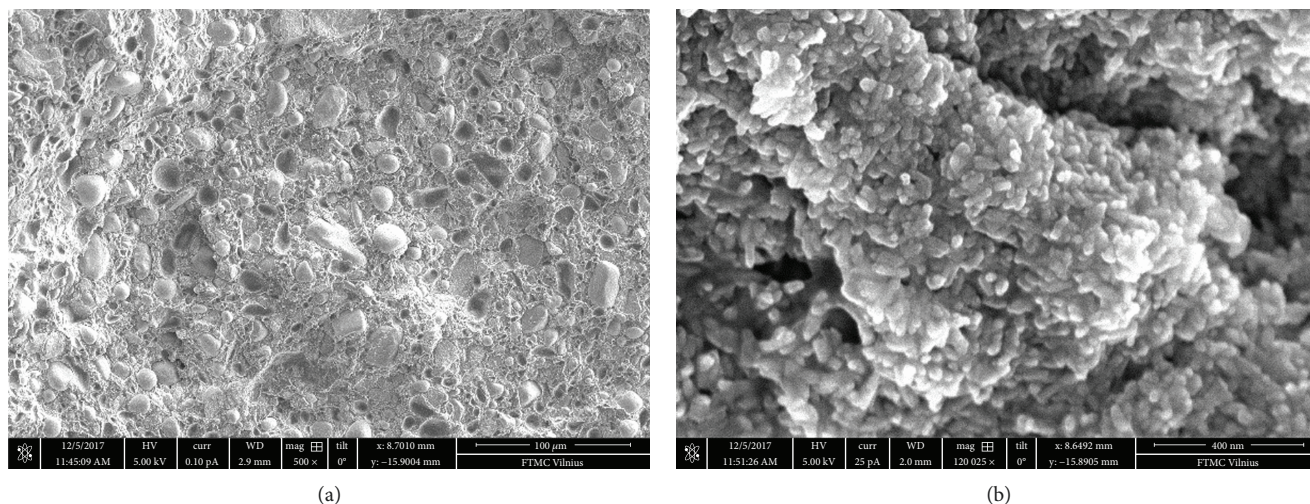


FIGURE 2: Scanning electron microscopy image of $\text{Fe}_2\text{O}_3\cdot\text{H}_2\text{O}$ Nanorods/epoxy composites with 40 vol.% filler concentration (at different magnification levels).

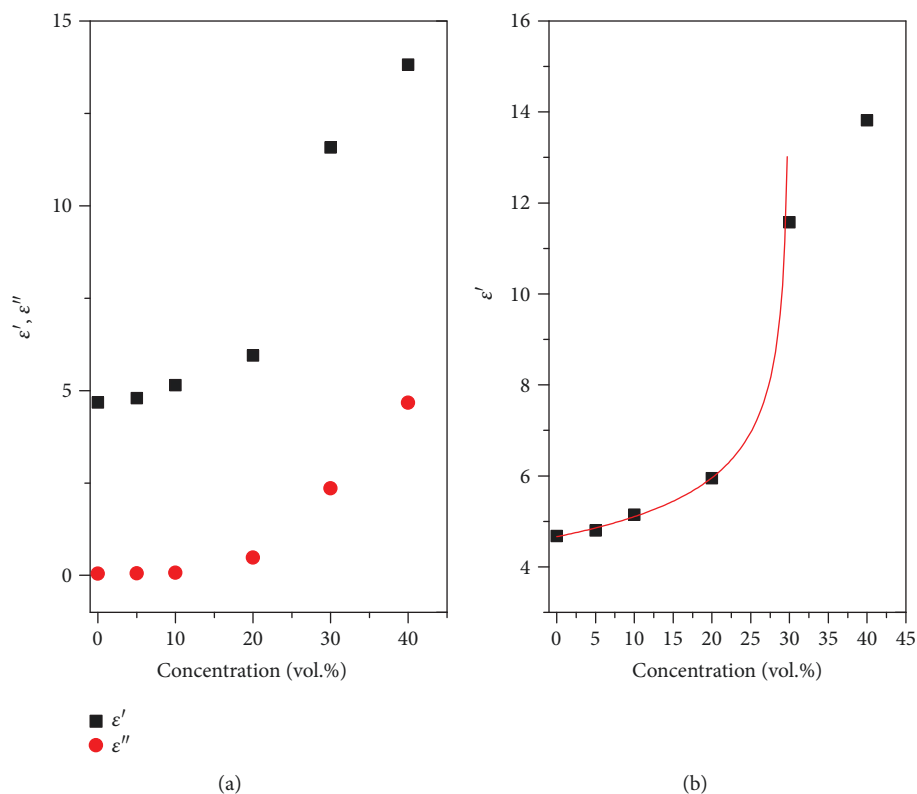


FIGURE 3: (a) Dependence of the complex dielectric permittivity of $\text{Fe}_2\text{O}_3\cdot\text{H}_2\text{O}$ /epoxy on filler concentration at room temperature and 129 Hz frequency. (b) A percolation law of the real part of permittivity $\epsilon \propto (30 - p)^{-0.24}$ for $\text{Fe}_2\text{O}_3\cdot\text{H}_2\text{O}$ /epoxy composites.

At high temperatures, the imaginary part of the dielectric permittivity increases strongly even for composites below the percolation threshold. Such behavior at high temperatures (above 400 K) is typical for epoxy resin composites [1] and is related to the phenomenon of electrical conductivity, which dominates in composites both above and below the percolation threshold. The temperature dependence of the complex dielectric permittivity at different frequencies for a

composite with 5 vol.% filler concentration is shown in Figure 5. The imaginary part of the dielectric permittivity presents a maximum, in which position is frequency-dependent. When the frequency increases, the maximum expands and shifts towards higher temperatures.

The real part of the dielectric permittivity decreases with increasing frequency. Such dielectric dispersion is typical for epoxy molecule dynamics [1]. At high temperatures (above

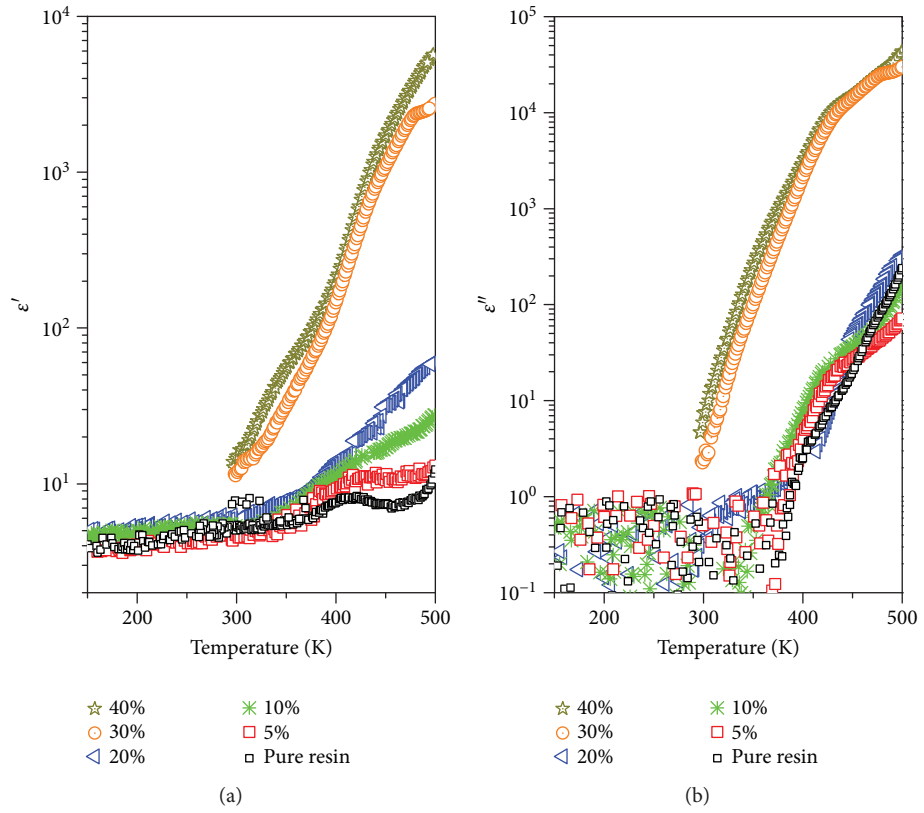


FIGURE 4: Temperature dependence of the complex dielectric permittivity of $\text{Fe}_2\text{O}_3 \cdot \text{H}_2\text{O}$ /epoxy composites at 129 Hz.

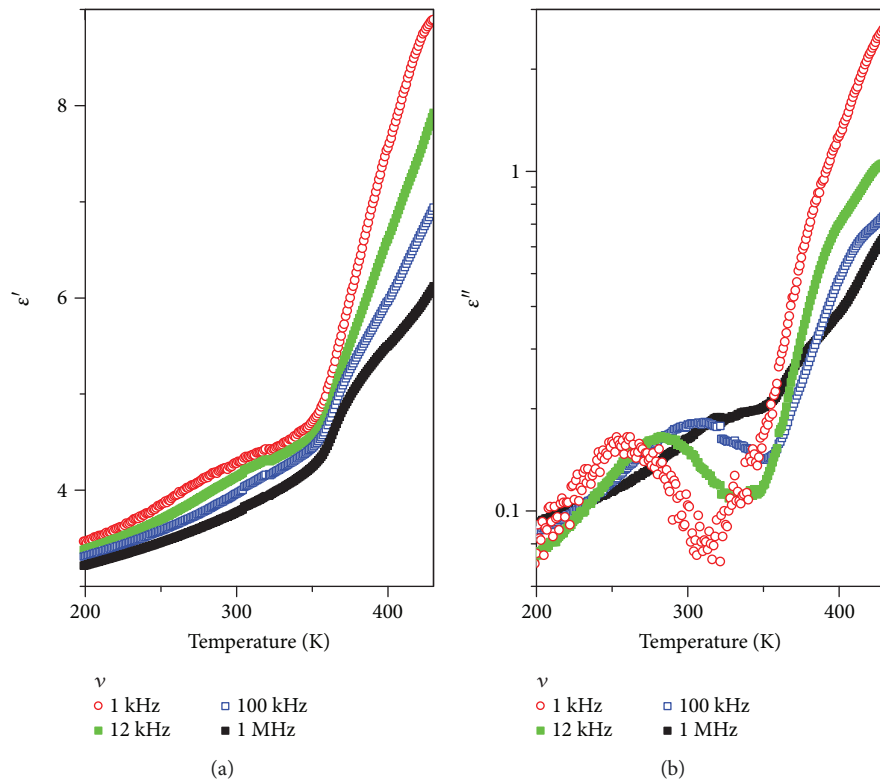


FIGURE 5: Temperature dependence of the complex dielectric permittivity of $\text{Fe}_2\text{O}_3 \cdot \text{H}_2\text{O}$ /epoxy composites with 5 vol.% filler concentration at different frequencies.

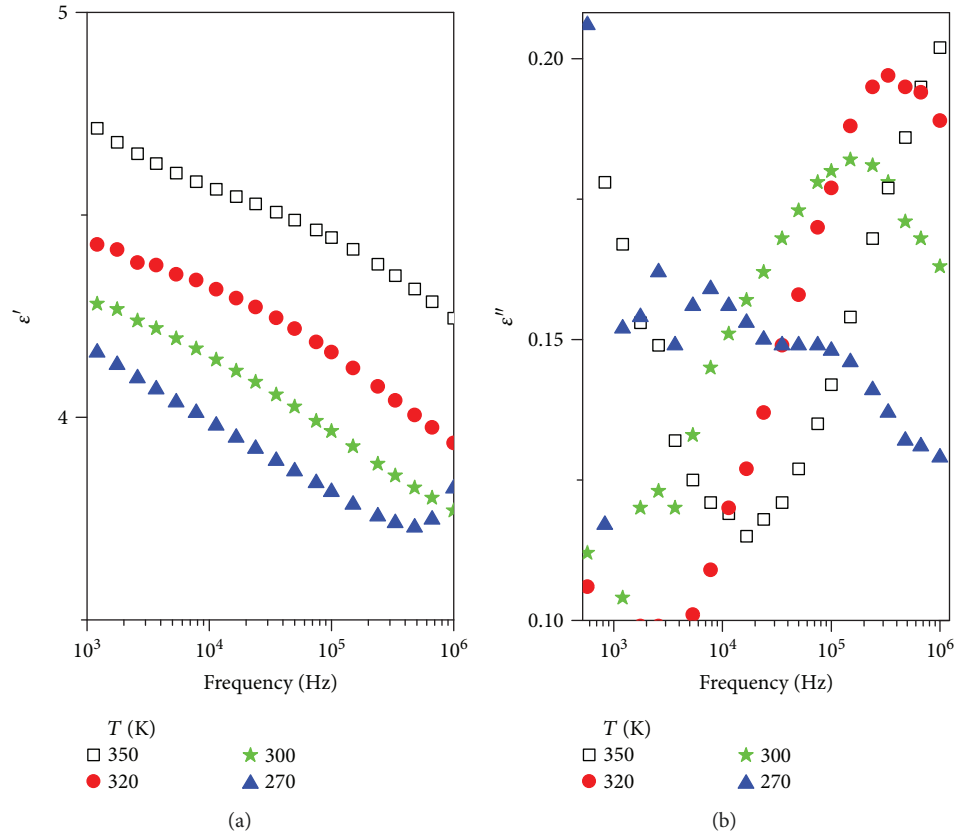


FIGURE 6: Frequency dependence of the complex dielectric permittivity of $\text{Fe}_2\text{O}_3\cdot\text{H}_2\text{O}$ /epoxy composites with 5 vol.% filler concentration at different temperatures.

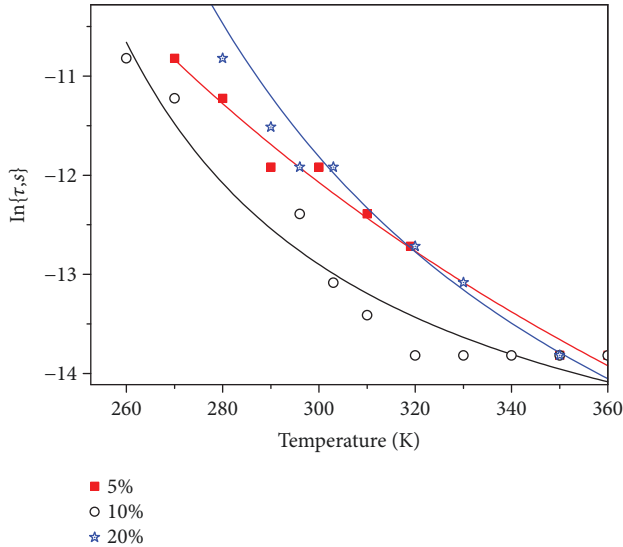


FIGURE 7: Temperature dependence of the average relaxation time of $\text{Fe}_2\text{O}_3\cdot\text{H}_2\text{O}$ /epoxy composites. The solid lines correspond to the approximations by Vogel-Fulcher law (see equation (1)).

350 K), the complex dielectric permittivity and the loss tangent ϵ''/ϵ' sharply increases due to the appearance of electrical conductivity.

TABLE 1: Parameters of the Vogel-Fulcher law fit of the average relaxation time.

Concentration (vol.%)	$\ln \{ \tau_0, s \}$	E_B/k_B (K)	T_0 (K)
0	-27.4	2689	142
5	-20	1649	91
10	-18	773	152
20	-18	805	180

3.3. Frequency Dependencies of Complex Dielectric Permittivity. The frequency dependence of the complex dielectric permittivity at different temperatures for $\text{Fe}_2\text{O}_3\cdot\text{H}_2\text{O}$ /epoxy resin composite with 5 vol.% filler concentration is shown in Figure 6. At temperatures above 25°C, the spectra of the imaginary part of the dielectric permittivity presents a maximum corresponding to the absorption peak. The physical process that causes the absorption peak is the reorientation of the dipoles. This behavior is typical for composites below the percolation threshold, and it is due to the dipole relaxation [18, 24].

On cooling, the maximum of ϵ'' expands and shifts towards low frequencies, while at low temperatures (below 270 K), it generally disappears. The frequency at the maximum of the imaginary part of the dielectric permittivity at a fixed temperature, ν_{\max} , allow us to determine the average

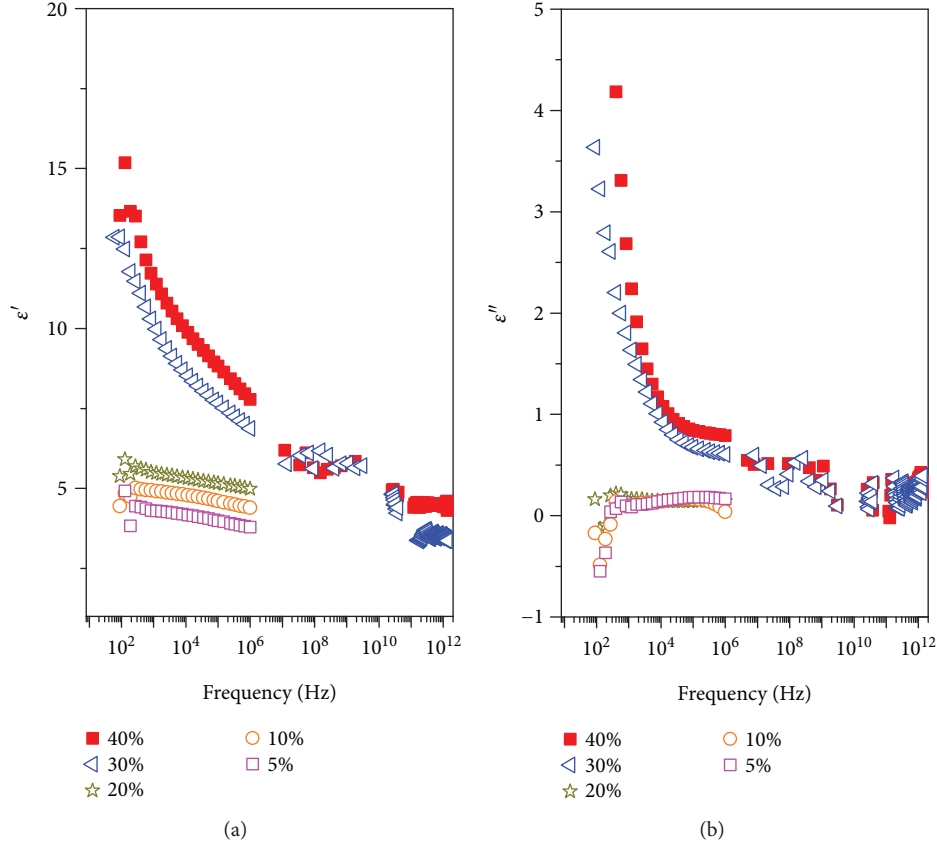


FIGURE 8: Room temperature broadband frequency dependence of complex dielectric permittivity of $\text{Fe}_2\text{O}_3\cdot\text{H}_2\text{O}$ /epoxy composites with different filler concentrations.

relaxation time by using the following equation: $\tau = 1/\nu_{\max}$. On cooling, the relaxation time increases according to the Vogel-Fulcher law (see Figure 7):

$$\tau = \tau_0 e^{(E_B/(k_B(T-T_0)))}, \quad (1)$$

where τ_0 is the relaxation time at very high temperatures, E_B is the activation energy, and T_0 is the glass transition temperature.

Obtained parameters are presented in Table 1. In composites, the glass transition temperature increases with goethite nanorod concentration. This increase can be explained by the strong interactions between epoxy resin and ($\text{Fe}_2\text{O}_3\cdot\text{H}_2\text{O}$) nanorods. Moreover, according to the theoretical calculations, the density of composite could be higher than the pure polymer density, and therefore the increasing of the glass transition temperature with the filler concentration could be observed [20].

The frequency dependence of the complex dielectric permittivity in a wide frequency range at room temperature is shown in Figure 8. The frequency range is wide (from hertz to terahertz). However, measurements above 1 MHz were performed only for composites above the percolation threshold (30 and 40 vol.%). This choice was due to the fact that the permittivity of composites below the percolation threshold at room temperature is almost frequency-independent and its value is close to pure epoxy resin permittivity [17, 20]. In

microwave frequency range, the value of complex dielectric permittivity is very similar to the corresponding properties of epoxy resin composites filled with iron nanowires and nanoparticles [11].

3.4. Electrical Conductivity. The electrical conductivity σ was calculated according to the following equation: $\sigma = \omega \epsilon_0 \epsilon''$, where $\omega = 2\pi\nu$, ν is the frequency, and ϵ_0 is the dielectric permittivity of vacuum. The frequency dependence of the electrical conductivity, $\sigma(\nu)$, for $\text{Fe}_2\text{O}_3\cdot\text{H}_2\text{O}$ /epoxy resin composite with 20 vol.% filler concentration at different temperatures (at temperatures not lower than 370 K, where any relaxation related to the polymer matrix is observed in dielectric spectra) is shown in Figure 9. In the investigated frequency range, two separate regions can be observed for electrical conductivity, namely, the region of the frequency-independent plateau (at low frequencies) and the frequency-dependent region (at high frequencies) [24]:

$$\sigma = \sigma_{\text{DC}} + A\omega^s, \quad (2)$$

where σ_{DC} is the DC conductivity and $A\omega^s$ is the AC conductivity. The DC conductivity is due to a random distribution of electrical charge carriers. The AC conductivity σ_{AC} increases, approximately, according to a power law with an almost equivalent slope. The conductivity spectra can be fitted with equation (2) very well, except the data at very low

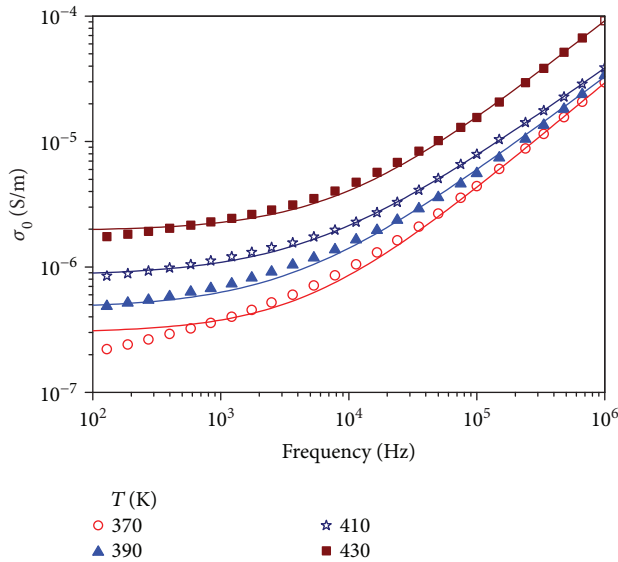


FIGURE 9: Frequency dependence of electrical conductivity of $\text{Fe}_2\text{O}_3\cdot\text{H}_2\text{O}/\text{epoxy}$ composites with 20 vol.% filler concentration at different temperatures. The solid lines are the best fit according to equation (2).

frequencies, where discrepancies appear due to blocking contact effects [25]. This behavior of both DC and AC conductivity can be addressed to the contribution of electronic conductivity inside epoxy resin [1]. A similar conductivity behavior was observed for all other investigated composites (see Figure 10) and has good agreement with the data presented in the literature for metal oxide composites [10], as well as for composites based on, for example, carbon filler [1, 16, 19, 26]. Another characteristic feature is an increase of the DC conductivity with the filler concentration (see Figure 10).

The temperature dependence of DC conductivity was approximated by the Arrhenius law:

$$\sigma_{\text{DC}} = \sigma_0 \exp\left(-\frac{E_A}{kT}\right), \quad (3)$$

where σ_0 is the preexponential factor and E_A is the conductivity activation energy. Obtained parameters are present in Table 2. In composites, the conductivity activation energy is almost independent from filler concentration below the percolation threshold, while above the percolation threshold, it decreases with filler concentration. Similar results are obtained for epoxy resin composites filled with carbon nanotubes and carbon black [1, 27].

Thus, at high temperatures, because of the finite conductivity of the epoxy resin, electrical conductivity occurs in composites both above and below the percolation threshold.

4. Conclusions

The dielectric properties of $\text{Fe}_2\text{O}_3\cdot\text{H}_2\text{O}$ nanorods/epoxy resin composites are presented in a wide frequency range from hertz to terahertz at temperatures of 200 K–450 K.

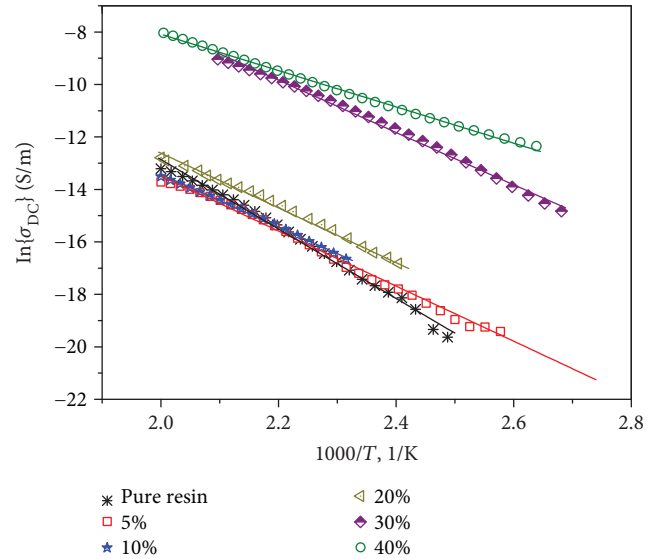


FIGURE 10: Temperature dependence of DC electrical conductivity of $\text{Fe}_2\text{O}_3\cdot\text{H}_2\text{O}/\text{epoxy}$ composites with different filler concentrations.

TABLE 2: Parameters of the Arrhenius law fit of the DC conductivity.

	σ_0 (S/m)	E_A/k_B (K)
Pure resin	$0.8 \cdot 10^6$	13225
5 vol.%	$0.2 \cdot 10^4$	10480
10 vol.%	$0.8 \cdot 10^3$	10073
20 vol.%	$0.4 \cdot 10^4$	10438
30 vol.%	$0.2 \cdot 10^6$	9973
40 vol.%	$0.3 \cdot 10^3$	6921

The percolation threshold of $\text{Fe}_2\text{O}_3\cdot\text{H}_2\text{O}$ nanorods/epoxy resin composites was about 30 vol%. The dielectric properties of composites below the percolation threshold are mainly determined by relaxation in a pure polymer matrix. The dielectric properties of composites above the percolation threshold are determined by the percolation network, which is formed by the filler particles inside the composite. At low frequencies, the DC conductivity is produced by the random distribution of electric charge carriers and increases with the concentration of inclusions. At high temperatures, because of the finite conductivity of the epoxy resin, the electrical conductivity occurs in the composites both above and below the percolation threshold.

Data Availability

The data used to support the findings of this study are available from the corresponding author upon request.

Conflicts of Interest

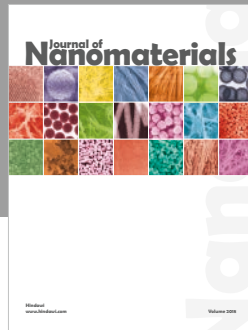
The authors declare that there is no conflict of interest regarding the publication of this paper.

Acknowledgments

This research was partly funded by H2020 RISE project 734164 Graphene 3D. D. Bychanok and P. Kuzhir are thankful for the support by Tomsk State University Competitiveness Improvement Program. This research was also partially supported by the Research Council of Lithuania according to the Lithuanian-Belarus Collaboration Program Project (no. S-LB-17-2/LSS-120000-143).

References

- [1] J. Macutkevicius, P. Kuzhir, A. Paddubskaya et al., "Epoxy resin/carbon black composites below the percolation threshold," *Journal of Nanoscience and Nanotechnology*, vol. 13, no. 8, pp. 5434–5439, 2013.
- [2] J. Macutkevicius, D. Seliuta, G. Valušis et al., "High dielectric permittivity of percolative composites based on onion-like carbon," *Applied Physics Letters*, vol. 95, no. 11, article 112901, 2009.
- [3] G. Inzelt, *Conducting Polymers: a New Era in Electrochemistry*, Springer-Verlag, Heidelberg, 2008.
- [4] K. J. Vinoy and R. M. Jha, *Radar Absorbing Materials: From Theory to Design and Characterization*, Kluwer Academic Publishers, Boston, 1996.
- [5] F. Qin and C. Brosseau, "A review and analysis of microwave absorption in polymer composites filled with carbonaceous particles," *Journal of Applied Physics*, vol. 111, no. 6, article 061301, 2012.
- [6] M. Fu, Y. Yu, J. J. Xie et al., "Significant influence of film thickness on the percolation threshold of multiwall carbon nanotube/low density polyethylene composite films," *Applied Physics Letters*, vol. 94, no. 1, article 012904, 2009.
- [7] K. Ahmad, W. Pan, and S.-L. Shi, "Electrical conductivity and dielectric properties of multiwalled carbon nanotube and alumina composites," *Applied Physics Letters*, vol. 89, no. 13, article 133122, 2006.
- [8] W. Bauhofer and J. Z. Kovacs, "A review and analysis of electrical percolation in carbon nanotube polymer composites," *Composites Science and Technology*, vol. 69, no. 10, pp. 1486–1498, 2009.
- [9] G. Y. Yurkov, S. P. Gubin, D. A. Pankratov et al., "Iron (III) oxide nanoparticles in a polyethylene matrix," *Inorganic Materials*, vol. 38, no. 2, pp. 137–145, 2002.
- [10] E. Temizel, E. Ayan, M. Şenel et al., "Synthesis, conductivity and magnetic properties of poly(N-pyrrole phosphonic acid)-Fe₃O₄ nanocomposite," *Materials Chemistry and Physics*, vol. 131, no. 1-2, pp. 284–291, 2011.
- [11] R. B. Yang, W. F. Liang, W. S. Lin, H. M. Lin, C. Y. Tsay, and C. K. Lin, "Microwave absorbing properties of iron nanowire at x-band frequencies," *Journal of Applied Physics*, vol. 109, no. 7, article 07B527, 2011.
- [12] M. Krajewski, W. S. Lin, H. M. Lin et al., "Structural and magnetic properties of iron nanowires and iron nanoparticles fabricated through a reduction reaction," *Beilstein Journal of Nanotechnology*, vol. 6, pp. 1652–1660, 2015.
- [13] M. Iacob, G. Stiubianu, C. Tugui et al., "Goethite nanorods as a cheap and effective filler for siloxane nanocomposite elastomers," *RSC Advances*, vol. 5, no. 56, pp. 45439–45445, 2015.
- [14] R. Mariño-Fernández, S. H. Masunaga, N. Fontañá-Troitiño, M. P. Morales, J. Rivas, and V. Salgueirino, "Goethite (α -FeOOH) nanorods as suitable antiferromagnetic substrates," *The Journal of Physical Chemistry C*, vol. 115, no. 29, pp. 13991–13999, 2011.
- [15] <https://www.us-nano.com/inc/sdetail/42381>.
- [16] D. Bychanok, G. Gorokhov, D. Meisak et al., "Design of carbon nanotube-based broadband radar absorber for Ka-band frequency range," *Progress In Electromagnetics Research M*, vol. 53, pp. 9–16, 2017.
- [17] D. Bychanok, P. Kuzhir, S. Maksimenko, S. Bellucci, and C. Brosseau, "Characterizing epoxy composites filled with carbonaceous nanoparticles from dc to microwave," *Journal of Applied Physics*, vol. 113, no. 12, article 124103, 2013.
- [18] S. Bellucci, L. Coderoni, F. Micciulla, G. Rinaldi, and I. Sacco, "The electrical properties of epoxy resin composites filled with Cnts and carbon black," *Journal of Nanoscience and Nanotechnology*, vol. 11, no. 10, pp. 9110–9117, 2011.
- [19] J. Grigas, *Microwave Dielectric Spectroscopy of Ferroelectrics and Related Materials*, Gordon and Breach Publishers, Amsterdam, 1996.
- [20] I. Kranauskaite, J. Macutkevicius, J. Banys et al., "Synergy effects in the electrical conductivity behavior of onion-like carbon and multiwalled carbon nanotubes composites," *Physica Status Solidi (B)*, vol. 252, no. 8, pp. 1799–1803, 2015.
- [21] D. van der Putten, J. T. Moonen, H. B. Brom, J. C. M. Brokken-Zijp, and M. A. J. Michels, "Evidence for superlocalization on a fractal network in conductive carbon-black-polymer composites," *Physical Review Letters*, vol. 69, no. 3, pp. 494–497, 1992.
- [22] S. Kirkpatrick, "Percolation phenomena in higher dimensions: approach to the mean-field limit," *Physical Review Letters*, vol. 36, no. 2, pp. 69–72, 1976.
- [23] Y. Deng and H. W. J. Blöte, "Monte Carlo study of the site-percolation model in two and three dimensions," *Physical Review E*, vol. 72, no. 1, article 016126, 2005.
- [24] A. K. Jonscher, "New interpretation of dielectric loss peaks," *Nature*, vol. 256, no. 5518, pp. 566–568, 1975.
- [25] J. Banys, J. Macutkevicius, V. Samulionis, A. Brilingas, and Y. Vysochanskii, "Dielectric and ultrasonic investigation of phase transition in CuInP₂S₆ crystals," *Phase Transitions*, vol. 77, no. 4, pp. 345–358, 2004.
- [26] H. M. Kim, M. S. Choi, J. Joo, S. J. Cho, and H. S. Yoon, "Complexity in charge transport for multiwalled carbon nanotube and poly(methyl methacrylate) composites," *Physical Review B*, vol. 74, no. 5, article 054202, 2006.
- [27] J. Macutkevicius, P. P. Kuzhir, A. G. Paddubskaya et al., "Broadband dielectric/electric properties of epoxy thin films filled with multiwalled carbon nanotubes," *Journal of Nanophotonics*, vol. 7, no. 1, article 073593, 2013.



Hindawi
Submit your manuscripts at
www.hindawi.com

